EXPLICIT ANALYSIS OF THE LATERAL MECHANICS OF WEBS TRANSITING CONCAVE ROLLERS

By

S. Vaijapurkar and J. K. Good
Oklahoma State University
USA

ABSTRACT

All previous analyses of webs encountering spreading devices have required enforcement of assumed boundary conditions. An example is the normal entry boundary condition which has been employed in many web/roller analyses. Explicit finite element analyses show much promise for studying all types of web handling problems. The primary benefit of this type of analysis is that only very basic assumptions are required, average web velocity and tension for example. Beyond this the interaction of webs with rollers are governed entirely by forces of contact and friction that develop between the web and rollers. Conditions of stick and slip are possible. Additional benefits include the ability to study web deformations and stresses which may reveal the boundary conditions that can be employed in models that are computationally less expensive.

This paper will focus on a study of the behavior of a web transiting a concave roller. It will be shown that a concave roller can be an effective spreader locally in the entry span as a web approaches a roller but can cause web instability in the form of troughs in an exit span. Results for several roller concavities, friction coefficients and web materials will be presented. Finally an assessment of when kinematic boundary conditions such as the normal entry condition are valid will be made.

INTRODUCTION

Concave rollers can be solutions to various web handling problems that result from widthwise web contraction. Troughs, wrinkles and baggy lanes can be visual identifiers of such problems but in some cases like that of nonwovens the width reduction may be absorbed by the web but the loss of width may still be unacceptable. Concave rollers have been employed with various levels of success. Several sources warn that too much concavity should be avoided and provide guidelines for limiting the diameter variation. One source limits diameter differences to 0.1% for high modulus webs and 0.5% for low modulus webs [1]. Another source [2] offers the algorithm $Y^2 = 180{,}000X$ where Y is half the roller width and X is the amount of material removed from the radius of the roller at

the center of the roller. The amount of material removed from the radius would decrease parabolically to zero at the edge of the roller. This expression requires units of inches in the example given. These limits are provided because the sources are aware that devices such as concave rollers are capable of creating web problems. Potential problems can include inducing nonuniform inelastic deformation in the web and lateral dynamic instability. The interaction between the web and the concave roller is not fully understood. Although the devices are useful, there is yet much to be explored about their working and design before they can be designed for particular applications. Experimentation is difficult since most accurate means of strain and stress measurement are interfering methods when applied to thin webs.

Theoretical investigation of webs encountering rollers with contoured profiles date back to Swift[3] who developed design guidelines for belts transiting tapered pulleys. Swift treated the belt as a beam that was subjected to moments that arose from the interaction of the belt and the tapered pulley. He was the first to recognize the normal entry rule and investigate various geometrical irregularities of shaft alignment, oblique drives and staggered pulleys. Delahoussaye and Good [4] studied effects of variations in geometry, material properties and operating conditions on concave and crowned rollers. They gave FE models predicting elastic deformation and stresses in web crossing these rollers. There are some interesting observations noted in their research including the existence of compressive CD stresses in exit span, which is consistent with findings of this work. Because they enforce no slip boundary conditions, their model assumes the deformations of web remain constant as the web passes over the concave roller. Swanson[5] presented results of testing several spreading devices. Although Swanson found the concave roller to be both an effective spreader and anti-wrinkling device he did not propose closed form or numerical solutions for designing concave rollers. Markum and Good[6], presented robust closed form solutions that an engineer can use to specify design parameters for two types of spreader devices. Starting with classical matrix analysis, they derived expressions for the MD stress distribution in the web and the spreading CD deformation of the web on roller. Their solutions assumed that the web upstream of the concave roller had troughs and wrinkles and thus the projected web width had become less than the planar web width under tension. The expressions they developed could be used to design concave rollers to return the web to a planar geometry in preparation for processing or handling operations that require the web to be planar (e.g. coating winding and laminating). Results from these expressions were verified by experiments. Algorithms were developed for the minimum operating tension to ensure full contact between the web and the concave roller and a maximum operating tension to prevent inelastic deformation of the web. Brown [7] proposed a new approach of analyzing webs using a conservation of mass rule and a new boundary condition called the normal strain rule. He assumes web as a stick zone on roller. His method employs a differential equation solver and he compared his results with experiments by Good[6] and Shelton[8].

Be it a classical theory or experimental analysis, all the authors discussed have spent a great deal of effort to understand web behavior on a concave roller. All of the works that develop analyses enforce assumed boundary conditions. These boundary conditions may be kinematic such as the normal entry law, kinetic boundary conditions such as no slip of the web on the roller or yet other conditions such as Brown's conservation of mass and normal strain rule.

The analyses presented herein have employed the explicit finite element method for solving problems of webs encountering contoured rollers. It can efficiently solve both transient and quasi-static problems. The contact algorithms are capable of modeling the

friction forces between web and rollers and determining when stick or slip will occur. Kandadai and Good [9] have already successfully analyzed problems of wound rolls using this method. Here they explained some basic concepts of material constitutive behavior, surface interaction, modeling and other computational aspects of this technique. No boundary conditions will be set in these analyses. If the traction between a web and roller is sufficient normal entry may be observable in the output. The web velocity and tension at the web ends, the web/roller friction coefficient, and the web elastic properties are the only conditions prescribed. When stick and slip occurs between the web and a roller it will be governed by Coulomb's Friction Model. The web properties and roller geometries are set to represent cases that have been reported in the literature.

EXPLICIT FINITE ELEMENT ANALYSIS

An explicit dynamic analysis is computationally efficient analysis tool. Large models having relatively short dynamic response times and discontinuous processes can be analyzed. Unlike implicit methods, there is no global stiffness matrix involved. The explicit central-difference operator satisfies the dynamic equilibrium equations at the beginning of the time increment *t;* the accelerations calculated at time *t* are used to advance the velocity solution to time *(t + Δt/2)* and the displacement solution to time *(t + Δt).* This analysis is suitable to study webs in transit in web process machinery because it can resolve complicated contact problems. Explicit schemes determine the solution without iteration. It explicitly advances the kinematic state from the previous increment. Even though it requires larger number of increments, the analysis is more efficient than standard methods. Explicit methods consume fewer system resources for large-scale models as compared to implicit methods.

The Explicit Method of Analysis

The central difference rule is used to integrate the equations of motion explicitly through time, using the kinematic conditions at one increment to calculate the kinematic conditions at the next increment [9]. At the beginning of the increment the dynamic equilibrium is solved in a manner where the nodal mass matrix *M,* times the nodal accelerations $\ddot{u}$, equals the total nodal forces (the difference between the external applied force *P*, and internal element forces, *I*) which can be expressed as $M\ddot{u} = P - I$. The acceleration initiating the current increment (time t) is

$$\ddot{u}\big|_{(t)} = (M)^{-1}.(P-I)\big|_{(t)} \qquad \{1\}$$

The acceleration calculations are simple since they employ a diagonal, lumped mass matrix; the mass matrix is readily inverted. The acceleration at any node is determined by its mass and the net force acting on it. This makes the nodal calculations very fast and economical in terms of computational cost. The accelerations are integrated through time using the central difference rule, which calculates the change in velocity keeping the acceleration constant. This change in velocity is added to the velocity from the middle of the previous time increment to determine the velocities at the middle of the current increment as

$$\dot{u}\big|_{(t+\frac{\Delta t}{2})} = \dot{u}\big|_{(t-\frac{\Delta t}{2})} + \frac{(\Delta t\big|_{(t+\Delta t)} + \Delta t\big|_{(t)})}{2}\ddot{u}\big|_{(t)} \qquad \{2\}$$

The displacement at the end of the increment is determined by adding the velocities integrated through time to the displacement at the beginning of the increment.

$$u\big|_{(t+\Delta t)} = u\big|_{(t)} + \Delta t\big|_{(t+\Delta t)} \dot{u}\big|_{(t+\frac{\Delta t}{2})} \quad \{3\}$$

This satisfies the dynamic equilibrium at the beginning of the increment, which leads to acceleration. Once the acceleration is calculated, velocities and displacements incremented through time. For this method to produce accurate results, time increments must be very small so that the accelerations are constant during increment. The small time increments results in large number of steps, but it does not hurt the overall efficiency of the system since most of the computation expense lies in the calculation of internal forces acting on the elements. The element stresses and forces are calculated based on element strains and constitutive relationships.

The steps of any explicit dynamic algorithm are given as follows [10]:

1. Nodal calculations.
   a. Dynamic equilibrium. $\ddot{u}_{(t)} = M^{-1} (P_{(t)} - I_{(t)})$
   b. Integrate explicitly through time.

$$\dot{u}\big|_{(t+\frac{\Delta t}{2})} = \dot{u}\big|_{(t-\frac{\Delta t}{2})} + \frac{(\Delta t\big|_{(t+\Delta t)} + \Delta t\big|_{(t)})}{2} \ddot{u}\big|_{(t)} \ldots Velocity \quad \{4\}$$

$$u\big|_{(t+\Delta t)} = u\big|_{(t)} + \Delta t_{(t+\Delta t)} \dot{u}_{(t+\frac{\Delta t}{2})} \ldots Displacement \quad \{5\}$$

2. Element calculations.
   a. Compute element strain increments $d\varepsilon$, from the strain rate $\dot{\varepsilon}$.
   b. Compute stresses from constitutive equations.

$$\sigma_{(t+\Delta t)} = f(\sigma_{(t)}, d\varepsilon) \quad \{6\}$$

   c. Assemble nodal internal forces $I_{(t+\Delta t)}$

3. Set $(t+\Delta t)$ to t and return to Step 1.

A FINITE ELEMENT MODEL OF A WEB SPREAD BY A CONCAVE ROLLER

ABAQUS/Explicit®, a commercial FE program for simulations, was employed in these analyses. The rollers in the following analyses are modeled as rigid analytical surfaces in Abaqus. This allows the geometries of the contact surfaces of the cylindrical and concave rollers to be defined continuously. The web is modeled as an elastic material.

Concave Roller Models

The nominal geometry of a web moving over a concave roller is shown in Figure 1. The specifics indicated in the figure are the basis for calculating the nodal locations, directions and deformations required by the model. The origin of the coordinate system is located at the center of the roller where the center line of the web and roller intersect.

Since the roller geometry is not a simple cylinder, the web material cannot conform to the surface of the roller without being strained and hence the web experiences a profile of MD strain with respect to the CMD similar in form to the roller radius profile. A variation in surface speed across the width of web results from the variation in radius.

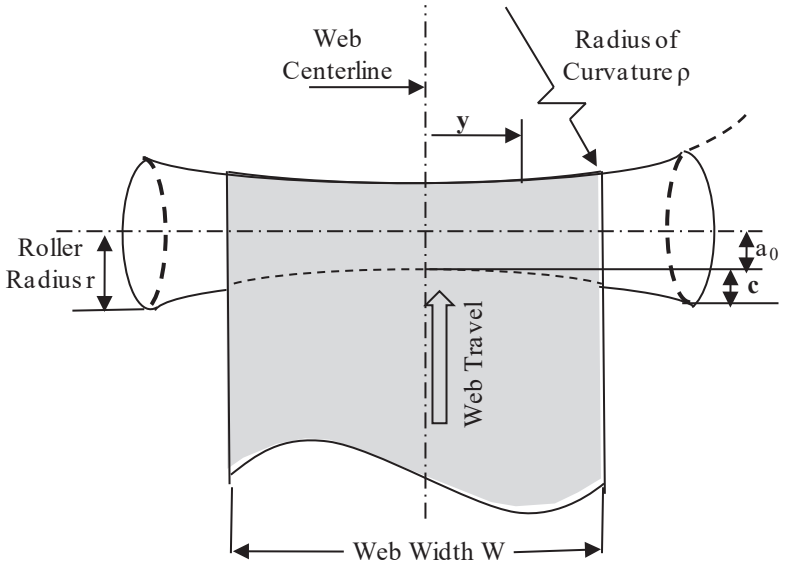

Figure 1 – Nominal Geometry and Configuration of Concave roller

The concave roller is modeled in the third position (R3) of a four roller setup as shown in Figure 2. Rollers R1, R2, and R4 are cylindrical rollers with a nominal radius of 36.8 mm (1.45 in.). The concave roller was modeled with three distinct concavities given in Table 1. The concavity is described per the method of Markum and Good [6] where the roller radius is prescribed by the expression $(r = a_o + a_1 y^2)$ where y is a CMD coordinate measured from the center location of the roller as shown in Figure 1.

Property	Values for Radius of Curvature ρ		
	ρ = 10.16 m	ρ = 15.24 m	ρ = 20.32 m
Parabolic roller profile coefficient a_0 *(mm)*	36.543	36.640	36.688
Parabolic roller profile coefficient a_1 *(1/mm)*	4.921E-5	3.281E-5	2.461E-5
Depression at the center *c (mm)*	0.287	0.191	0.142
End Radius *(mm)*	37.052	36.997	36.939

Table 1 – Geometrical Properties of Concave Rollers

All the four rollers are free to rotate around their longitudinal axis. The simulations are completed typically in twenty time steps. The first step consists of applying a known value of uniform tension load at the upstream end of the web while the downstream end

is restrained at zero velocity. In the second time step a prescribed value of MD velocity is set at the downstream end of the web for the remaining time steps. During the first time step as web tension develops, contact pressures also develop between the web and rollers. When the web begins moving in the second time step friction forces between the web and rollers begin to turn the rollers, much as any idler roller would be driven by a web. No kinematic boundary conditions between the web and rollers are enforced with the exception that the web is prevented from penetrating the rigid analytical roller surface by the contact algorithm. Only friction forces between the rollers and web dictate the lateral behavior of the web.

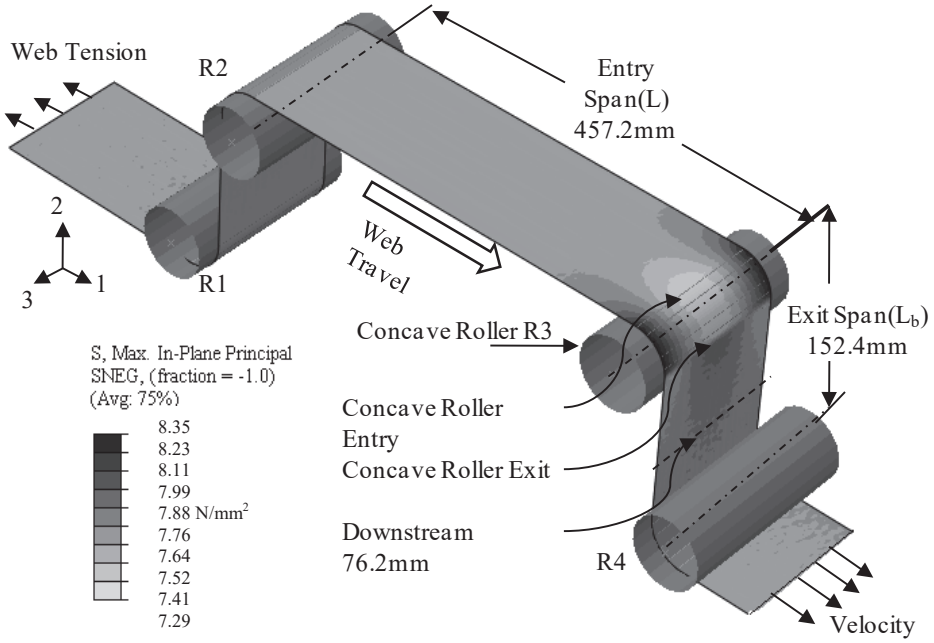

Figure 2 – Model Setup and Stress Locations for Concave Roller Analysis

Modeling the Web

Webs are similar to structures in which one dimension (the thickness) is significantly smaller than the other dimensions and the stresses in the thickness direction are negligible. There are Shell and Membrane elements in the element library from ABAQUS that resemble closely to this kind of behavior. Both kinds of elements are explored on various grounds for their suitability for modeling webs. General purpose shell elements could be used with finite strain and reduced integration selections since they account for finite membrane strains, arbitrarily large rotations, and these elements allow transverse shear deformation. The stress, strain, and other selected output variables are available at three section points through the depth of the element including the bottom and top surfaces and the mid-plane.

Membrane elements are surface elements that transmit only in-plane forces. They cannot react any moment and have no bending stiffness defined. A potential benefit of shell elements over the membrane elements is that with 6 defined degrees of freedom per node the out-of-plane deformation within the domain of an element can be more complex than the membrane elements. The benefit lies in that the contact between the web and surface of complex geometry such as the concave roller can be described with greater accuracy for a given mesh density. Membrane elements are computationally economical since they have fewer degrees of freedom per node to resolve.

Computation

The concave roller models consist of total with 60428 Elements and 149380 Nodes. An HP Workstation® with an Intel® Xeon® CPU processor with a speed of 3GHz and 3 GB of RAM were used for this simulations. The base parameters for study of concave rollers with explicit simulations are chosen such that it matches web materials and equipments used in web handling industry. Various parameters of the models are shown in Table 2. Solution times were nominally 60 hours. During these simulations about 127 cm (50 in) of web would pass over the four rollers.

Property	Value
Web Width *(W)*	152.4 mm (6 inch)
Web Thickness *(h)*	0.0234 mm(0.00092 inch)
Young's Modulus *(E)*	138N/mm^2(20000 psi)
Poisson's Ratio *(υ)*	0.3
Entering Span to concave roller *(L)*	457.2mm (18 inch)
Pre-entering span *(L_a)*	152.4mm (6 inch)
Web Tension *(T)*	1.75 N/cm (1pli)
Roller Radius *(r)*	36.8mm (1.45 inch)
Wrap Angle *(β)*	1.57rad (90 degrees)
Web Velocity *(v)*	12.7mm/sec(0.5 inch/second)
Coefficient of Friction *(μ)*	0.5

Table 2 – Concave Roller Model Parameter Values

FINITE ELEMENT MODEL RESULTS

Discussion

The concave roller has a higher surface velocity at the web edges than at the web center due to the larger radius at the web edges. If friction is sufficient that the web can attain the variation in surface velocity of the roller which will induce higher MD strains and stresses at the web edges with respect to the web center. Markum *et al* developed a closed form expression for calculating MD stress *(σ_{md})* related to MD strain *(ε_{md})* from uniaxial Hooke's law. They chose to do this since they assumed they were spreading a web that had laterally collapsed back to a planar form. This expression relates the stress at any point where the web enters the concave roller with the CMD distance of that point from the centroidal axis of web. Since the CMD centers of the web and concave roller are assumed to coincide, the stress distribution is symmetrical about the centroidal axis:

$$\sigma_{MD}(y) = E\frac{a_1(y^2 - W^2/12)}{a_0 + a_1 W^2/12)} + \frac{T}{h} \quad \{7\}$$

The largest MD stress occurs at the web edge (y=W/2) and is due both to the concave roller and the web tension (T):

$$\sigma_{MD}(W/2) = \frac{2Ea_1W^2}{12a_0 + a_1W^2} + \frac{T}{h} \quad \{8\}$$

A comparison of stress values induced by this relation with those results obtained from ABAQUS is shown in Figure 3. This comparison is for stresses at the edge of web at the entry point where the web first contacts the concave roller. The results shown in Figure 3 are in good agreement but stem from different assumptions or lack thereof. Expression {8} was derived assuming the web attained the velocity of the roller at the entry point, hence no slip. The Abaqus simulations incorporate no such assumption. Note that where deviation does exist that the Abaqus result is less than the result given by expression {8} which suggests some slip may exist.

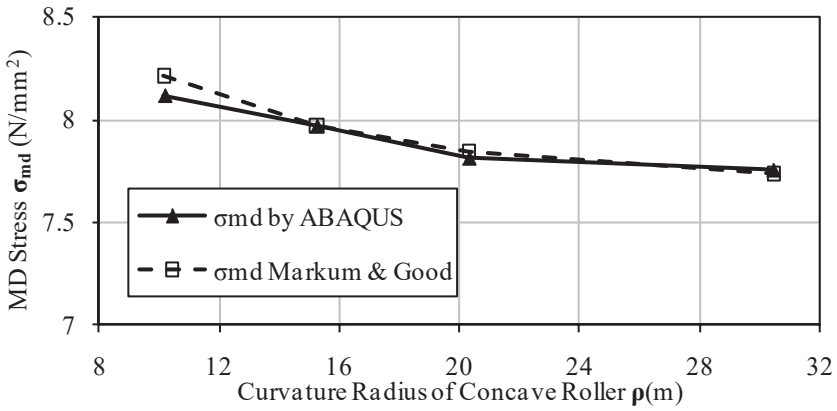

Figure 3 – Comparison of MD stress Induced by Concave Roller

The MD stress at entry and exit locations is shown as a function of CMD position in Figure 4. These stresses are compared with Markum and Good's model as explained earlier. It is obvious from the charts that the web undergoes a reversal of MD stresses as it travels from the roller to next free span. It also appears that the MD stress profile is not greatly affected by the radius of curvature of the roller. The impact is larger than appears here since the mean level of web stress due to tension is large compared to the variation caused by the concavity. The location of point of stress reversal occurs somewhere on the roller surface and must be accompanied by slippage.

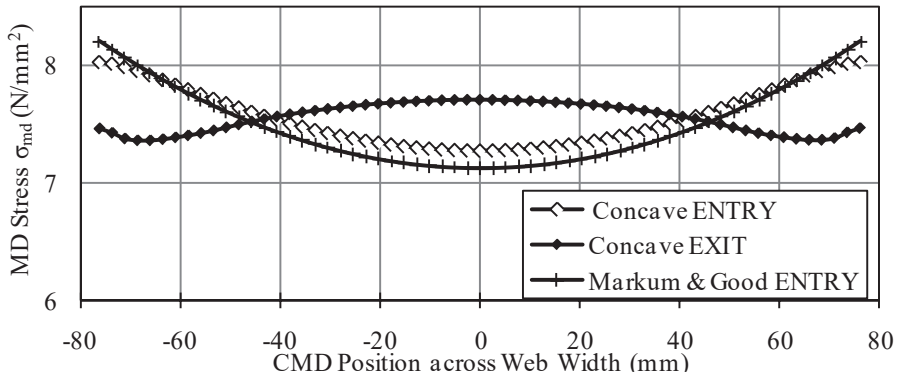

a) Roller Curvature Radius **ρ = 10.16m**

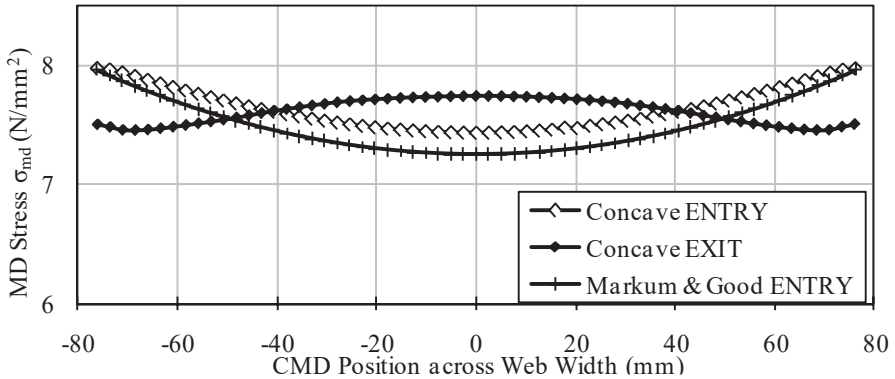

b) Roller Curvature Radius **ρ = 15.24m**

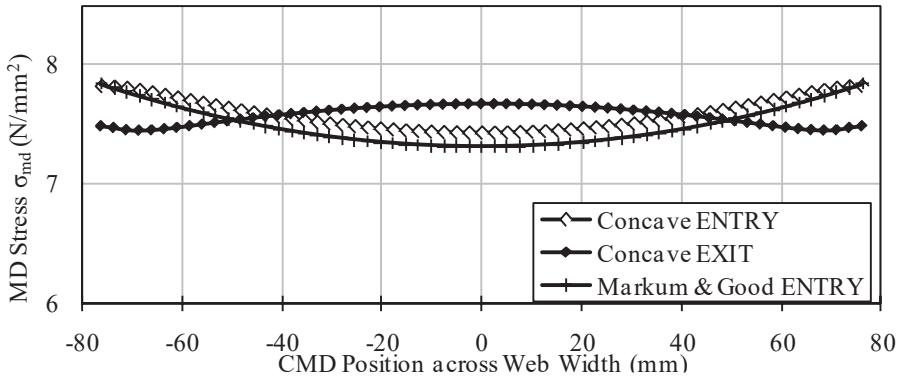

c) Roller Curvature Radius **ρ = 20.32m**

Figure 4 – MD Stress Variation as a Function of Curvature Radius at Entry and Exit of Concave Roller

Previous research conducted by Delahoussaye et al [4] was based on an enforced boundary condition of no slip. With such an assumption the MD stress variation seen in the CMD at the entry of the roller would have remained unchanged until the web exited the roller. The Abaqus simulations include no such assumption and it is obvious from

Figure 4 that for the cases studied that a no slip assumption may only be valid for a partial wrap of web on roller. To further study the MD stress variation occurring in the web transiting the concave roller the charts of Figure 5 are offered where the MD stress distribution along the centerline and the edge is shown. The line of observation starts approximately 203mm (8 in) upstream, proceeds in the MD to the concave roller, transits the roller and finally ends 76.2 mm (3 in) downstream of the concave roller exit.

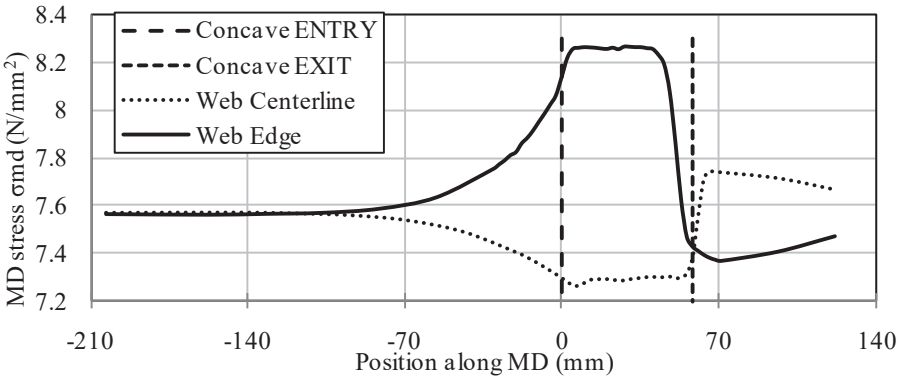

a) Roller Curvature Radius **ρ = 10.16m**

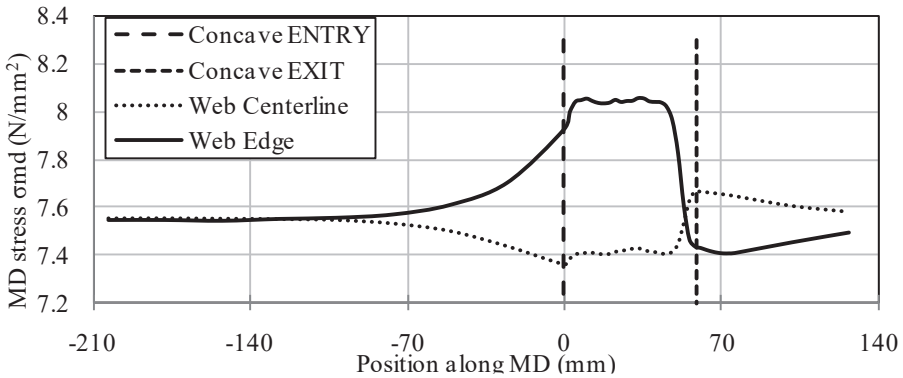

b) Roller Curvature Radius **ρ = 15.24m**

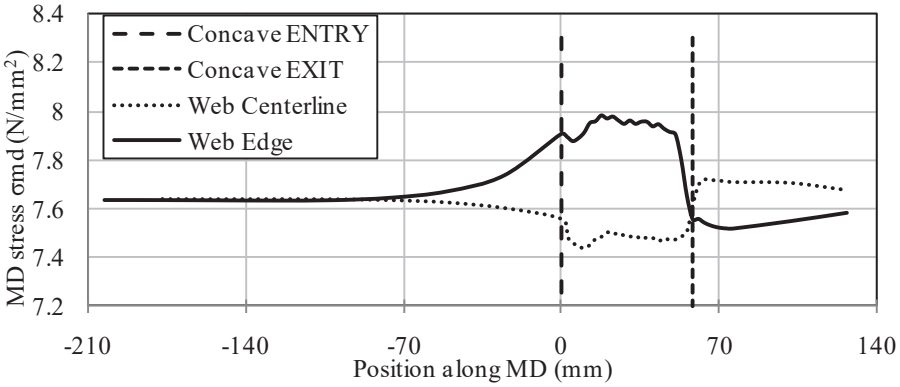

c) Roller Curvature Radius **ρ = 20.32m**

Figure 5 – MD Stresses on Edge and Centerline of Web Transiting Concave Roller

The charts indicate the MD stresses undergo change as the web passes over the roller and that an assumption of no slip would be unreasonable for the cases studied. Also these charts indicate the maximum MD stress at the web edge does not exist at the entry of the web to the roller but partially through the angle of wrap. The MD stresses are seen suddenly dropping near exit of roller. This is yet another indication of slip but is additional evidence that assumptions used in earlier analyses [4,7] are not always valid.

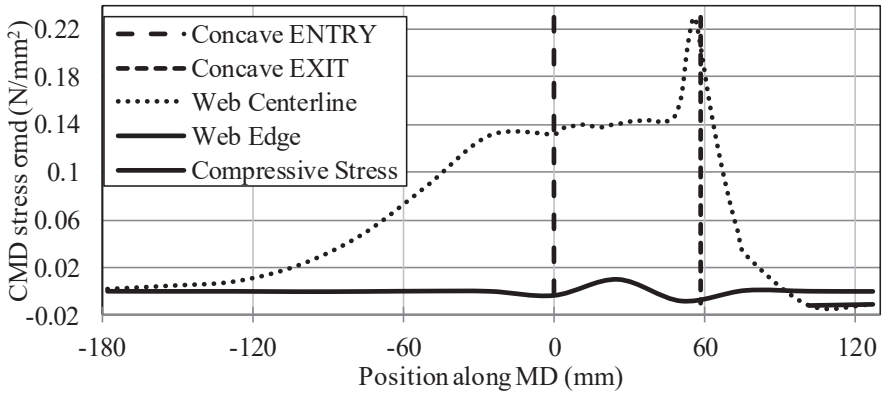

a) Roller Curvature Radius **ρ = 10.16m**

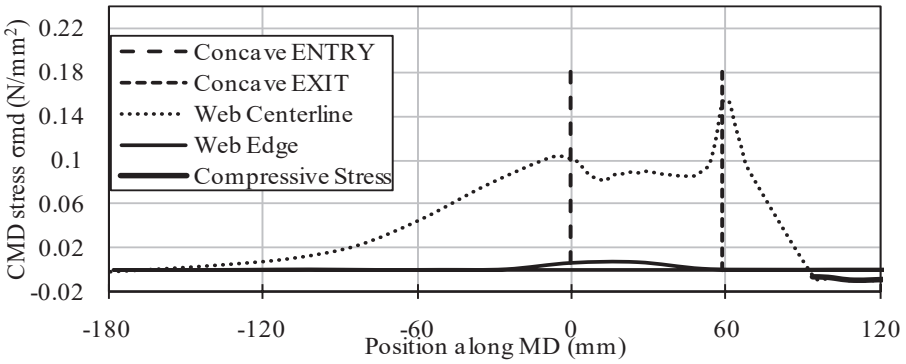

b) Roller Curvature Radius **ρ = 15.24m**

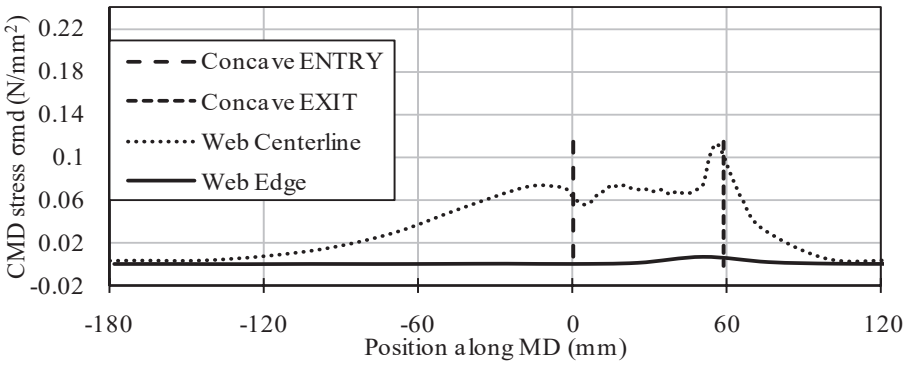

c) Roller Curvature Radius **ρ = 20.24m**

Figure 6 – CMD Stresses on Edge and Centerline of Web Transiting Concave Roller

Similar charts of the CMD stresses are shown in Figure 6. The largest CMD spreading stresses are witnessed on the centerline of the web. These stresses decrease towards the web edges where they become zero as required by surface equilibrium. The charts in Figure 6 show the CMD spreading stresses, on the web centerline, rise as the web approaches the entry to the concave roller. They then remain constant or decrease slightly and then rise to a peak as the web exits the roller. These peaks at the exit are the result of the rising MD stresses that were seen on the web centerline in Figure 5. The rising MD stress will result in a contracting strain in the CMD direction due to the Poisson effect. The contraction of the web is restricted by CMD friction forces near the exit resulting in an increase in the CMD stress. After exiting the roller the tensile spreading stress decreases and then becomes negative. Webs can react very little compressive CMD stress without buckling and forming web troughs. The appearance of compressive stresses in the exit section on the web center line was reported by previous researchers [4] too. Thus a device that is employed to spread webs can also be responsible for buckling the web in the exit span.

The development of negative CMD stresses in the exit span of the concave roller was explored further. The CMD stress output was used to produce charts of CMD stress versus CMD location at the entry and exit of the concave roller and then at a downstream location in Figure 7. Again the CMD spreading stresses in the web are shown to increase between the entry and exit of the concave roller. Note the CMD stresses in the web at the exit of the roller are tensile at the centerline but become negative (compressive) as the web edges are approached where they finally decline to zero. But also note that midway through the exit span (76.2 mm or 3 in downstream of the concave roller exit) the CMD stresses are negative and small. Also note that these stresses undulate slightly near the web centerline.

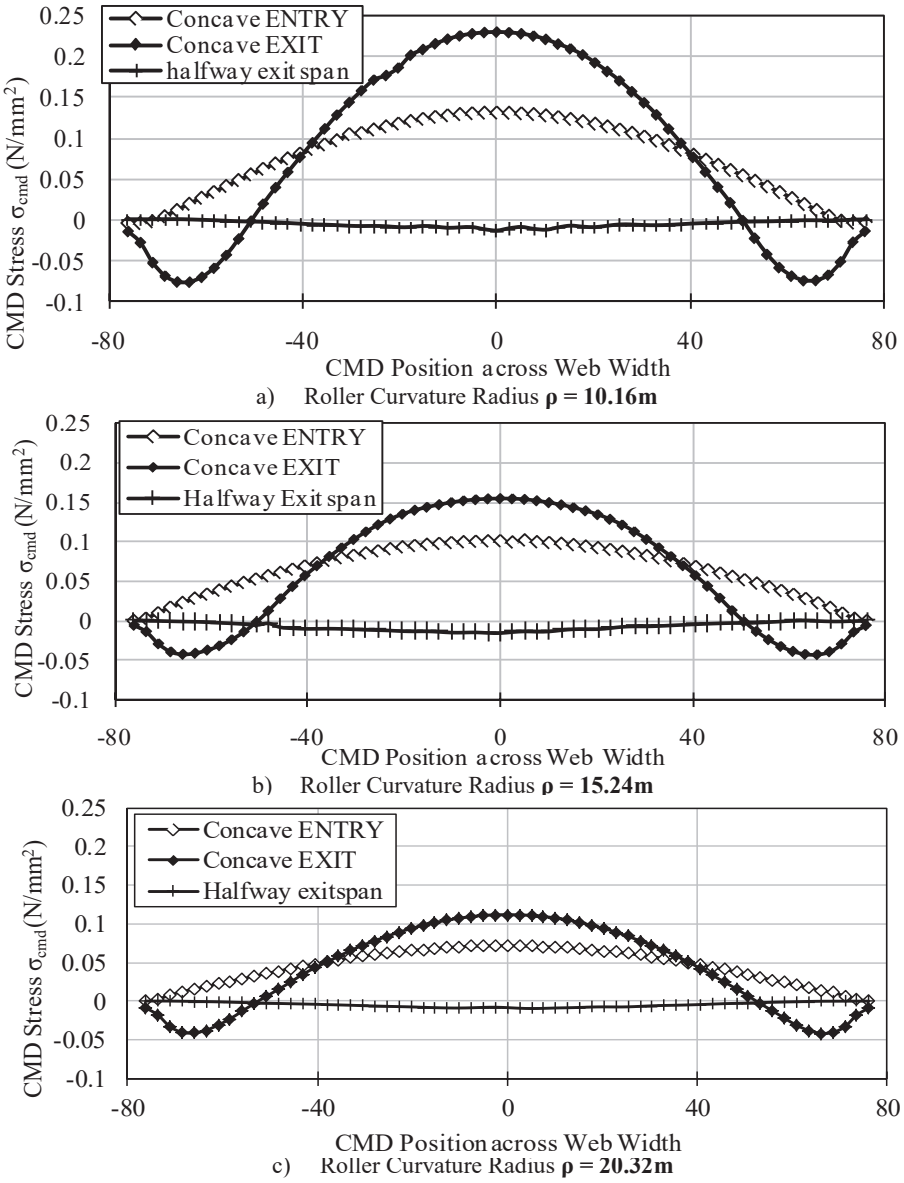

Figure 7 – CMD Stresses across the Width of Concave Roller. Compressive CMD Stresses Developed at Halfway Exit Span

Beisel *et al* [12] developed an expression for the value of critical negative CMD stresses in which will induce troughs in an isotropic web. If the stresses are more negative than this critical value, troughs will occur. The expression for the critical stress is:

$$\sigma_{ycr} = -\frac{\pi h}{\sqrt{3}a}\sqrt{\frac{\sigma_{MD}E}{\left(1-\nu^2\right)}} \qquad \{9\}$$

where h is the web thickness and a is the span length. For the web properties given in Table 2 and an exit span length of 152.4mm (6in) a critical buckling stress of -0.0094N/mm^2 is produced using expression {9}. Note the minimum CMD stresses seen in the exit span in Figure 7 are never less than -0.01 N/mm^2. This is indicative that buckling has occurred. When webs buckle into a troughed shape the wavelength λ or the distance between the trough crests can also be predicted. Again from Beisel *et al* [12]

$$\lambda = \frac{2a}{\sqrt[4]{1+\frac{\sigma_x}{\sigma_e}}} \quad \text{where } \sigma_e = \frac{\pi^2 D}{a^2 h} \text{ and } D = \frac{Eh^3}{12(1-\nu^2)} \qquad \{10\}$$

For an exit span length (L_b) of 15.24 cm (6 in) and for the web properties from Table 2 a wavelength of 7.62 mm (0.30 in) is calculated. In Figure 8, traces of the CMD surface stress on the bottom web surface and the out-of-plane deformation across the web width are shown for the case of curvature radius (ρ) 10.16m (400 in). These traces are shown since they exhibit evidence of the troughs and their wavelengths. While the wavelength calculated does not exactly match the wavelength shown in Figure 8, it does fall within the realm of modeling error since the element size is 2.54 mm.

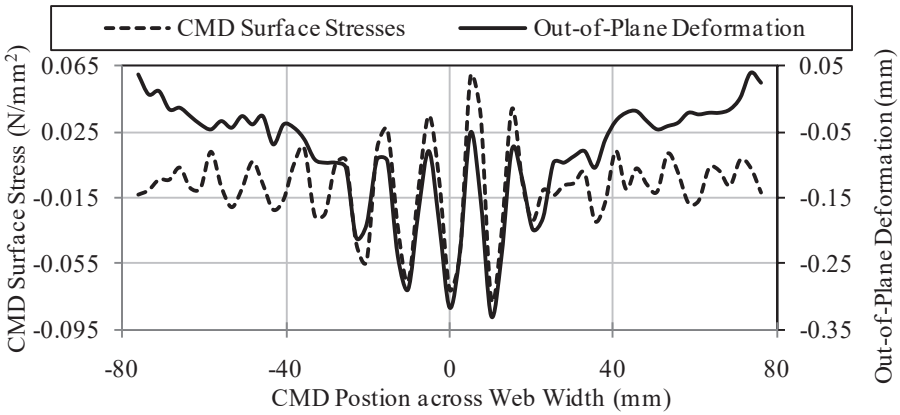

Figure 8 – Trough Behavior in CMD Surface Stress and Out-of-Plane Deformation for Curvature Radius **ρ = 10.16m**

Comparison of Membrane and Shell Elements

A comparison of results for the case where the curvature radius is 15.24m (600 in) obtained by both, the membrane and shell element is presented in Figure 9. Both types of elements yield very similar results. The MD and CMD stress profiles show exactly the same behavior. CMD spreading stresses are shown at the entry of the concave roller which increase at the web center as the web exits the roller. Also small regions of compressive CMD stress are seen near the web edges as the web exits the roller. As

stated earlier, membranes are computationally efficient and hence give output faster than shell elements of the same mesh density. The results presented here are mainly obtained from using the shell element since the concave roller geometry is anticlastic in shape, requiring the bending of an element around both axes of the shell.

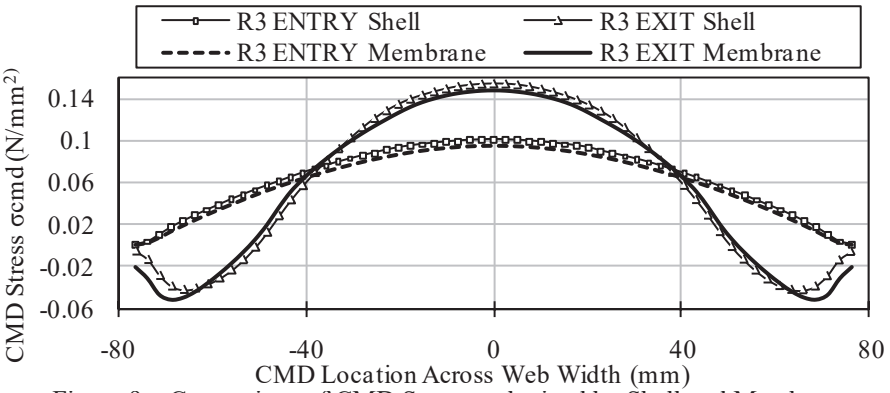

Figure 9 – Comparison of CMD Stresses obtained by Shell and Membrane Element across the Width of Roller.

Friction Forces

Web tension is responsible for the development of normal pressure between the web and roller surfaces. The web, while in contact with the roller can transmit shear as well as normal forces across the contact interface. The relationship between these forces is a cause of the stresses at the interface dictated by friction. The friction in the present modeling is governed by Coulomb friction model. This model assumes that no relative motion occurs if the equivalent frictional stress, τ_{eq} is less than the critical frictional stress τ_{crit} given by the friction coefficient μ times the contact pressure p. A plot of the shear contact stresses in MD and CMD (CShear1 and CShear2 in Abaqus) across the width of roller is presented in Figure 10. The values of contact shear stress extracted for the plots are at the exit location of the case where the roller radius of curvature was 15.24m (600in). The behavior of the contact shear stress can be linked to the MD and CMD stress profiles across the web width shown in Figures 4 and 7, respectively. As stated earlier the web exits roller with rising MD stresses at the center than that of the edges of web. It causes a contraction due to Poisson's effect in CMD. This contraction is limited by the shear contact stresses in the CMD which are shown in the figure.

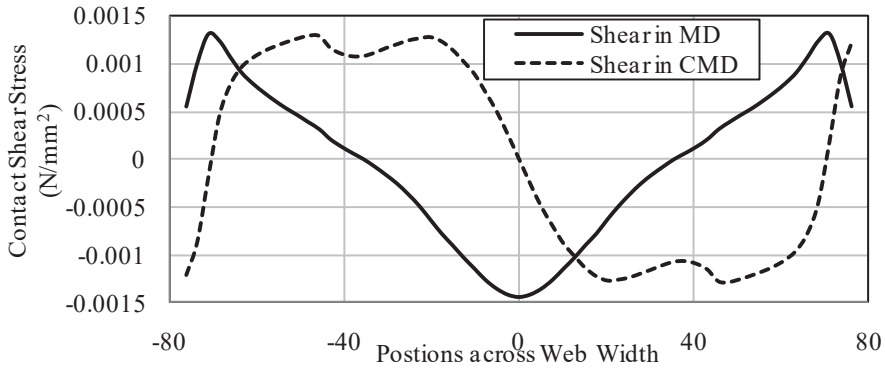

Figure 10 – Contact Shear Stress Distribution in MD and CMD across Web Width at the Exit of Concave Roller **ρ = 15.24m**

A CASE STUDY OF A WIDE WEB TRANSITING A CONCAVE ROLLER

The results presented so far might also be described as "Narrow" web results as many webs of much larger width are transported in process machines. The results were studied for concave rollers and webs that were typical of an earlier study [6]. Now a model will be developed for a case that was originally presented by Brown[13]. In this case the web is much wider and the span ratio has decreased markedly (L/W = 0.4). In addition the web modulus has increased. All of the parameters for this case are listed in Table 3.

A Wide Web Model

The model used for studying wide web is very similar to the model described earlier except the geometries, web properties and application of load. The concave roller is placed at the R3 location. The web is laid flat in the beginning of the simulation with R1 and R4 at its final position. R2 and R3 are vertically below the web but at their final locations in the 1 direction. This allows the model of the web to be defined with uniform web length prior to the beginning of the simulation. The first step consists of applying a known value of uniform tension load at the upstream end of the web while the downstream end is restrained at zero velocity. Rollers R2 and R3 are then moved into their final vertical positions in the second step. The web velocity is enforced at the downstream end of the web after a lapse of nearly 5 seconds. This time was given to allow the web out-of-plane dynamic motion to cease which was due to moving rollers R2 and R3 into position. When the web begins moving, the friction forces between the web and rollers begin to turn the rollers, much as any idler roller would be driven by a web. For these simulations again no kinematic boundary conditions between the web and rollers were enforced. Only friction forces between the rollers and web dictate the lateral behavior of the web. The base parameters for study of concave rollers with explicit simulations are chosen such that it matches web materials and equipments used in Brown's study. Various parameters of the models are shown in Table 3. The concave roller had a depression of 0.127mm (0.005 in) at its center. A web length of 137 cm (54 in) passed over the four rollers during the simulation.

Property	Value
Web Width *(W)*	1524 mm (60 inch)
Web Thickness *(h)*	0.0127 mm(0.0005 inch)
Young's Modulus *(E)*	4137 N/mm^2(600,000 psi)
Poisson's Ratio *(υ)*	0.35
Entering Span to concave roller *(L)*	610mm (24 inch)
Exiting span *(L_b)*	610mm (24 inch)
Web Tension *(T)*	0.875 N/cm (0.5pli)
Roller Radius *(r)*	76.2mm (3 inch)
Wrap Angle *(β)*	1.57rad (90 degrees)
Web Velocity *(v)*	15.24mm/sec(0.6 inch/second)
Coefficient of Friction *(μ)*	0.5

Table 3 – Concave Roller Model Parameter Values for Wide Web Study

Figure 11 shows the convergence of the MD stresses at the centerline and the edge of the web and also the CMD stresses at centerline of web during the simulation. Each simulation runs for 100 seconds of total time. The processes of web tension building and bringing the web to velocity occur in the first 5 seconds. The remainder of the simulation time is spent bringing the MD and CMD stresses to converged values. The MD stresses stabilize sooner than the CMD stresses in this case.

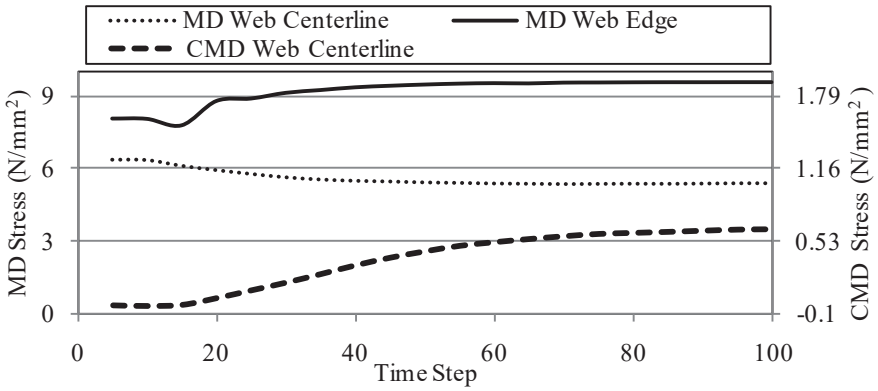

Figure 11 – Convergence of MD and CMD Stresses in Wide Web over the Total Step Time at the Entry of Concave Roller

WIDE WEB MODEL RESULTS

The results of the ABAQUS simulations were compared with stress values communicated by Brown [7]. The modeling parameters were input to the closed form solution {7} given by Markum and Good in their paper [6]. The distributions for the MD and CMD stresses are shown across the web width in Figure 12. The values match very well from these two independent sources and show very similar trends. As expected the web is undergoing an MD stress reversal as it exits the wide concave roller. The CMD stresses calculated by Browns code are slightly higher values than Abaqus presumably since he assumes no slip on the roller.

Also note the MD and CMD stresses have been shown at the exit of roller R2 which is also the beginning of the entry span of the concave roller. Often the ability of a spreader roller is limited by the length of the entry span. The MD stress variation induced by the concave roller R3 is sufficient in this case to cause MD and CMD stress variation at the exit of roller R2. This is an example where there could have been benefit in making the entry span longer. This would have allowed uniform MD stress and zero CMD stresses at the exit to R2 and there would thus be no slippage at the exit of roller R2. Herein the focus has been to study how a concave roller affects a planar web. These devices are often used to spread webs that have laterally collapsed or compacted. Markum et al [6] showed the spreading ability for such webs was proportional to the square of the entry span length.

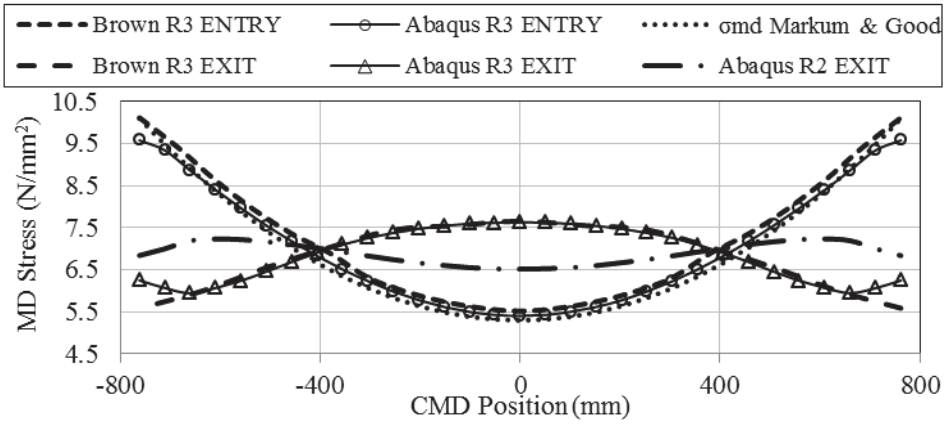

a) MD Stress Distribution for **c = 0.127mm (0.005in)**

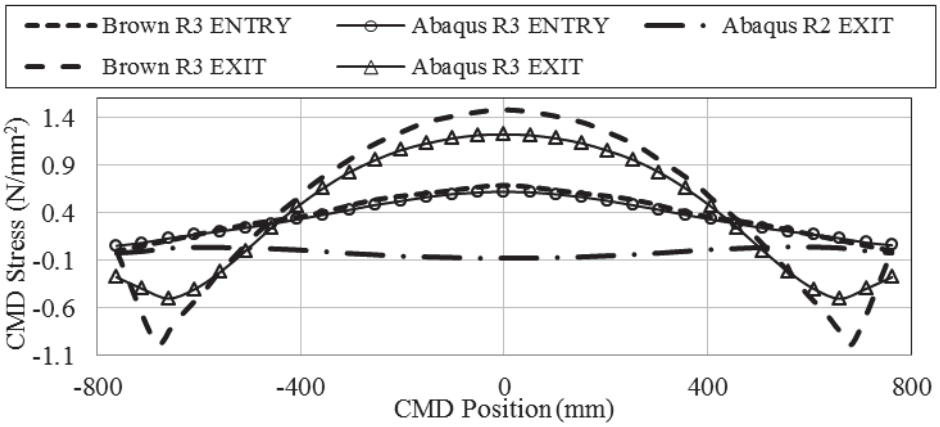

b) CMD Stress Distribution for **c = 0.127mm (0.005in)**

Figure 12 – Comparison of MD Stresses for Brown's Setup at Entry and Exit of Concave Roller.

Potential Kinematic Boundary Conditions

In the development of the models for both the narrow and wide webs it has been emphasized that no kinematic boundary conditions have been enforced that would affect the lateral deformation of the web. Now the lateral deformations will be examined to determine if some kinematic boundary conditions may be applicable. The wide web model results will be used in this case. Lateral deformations were harvested from several MD locations and the slope or derivative of those deformations were taken with respect to the MD coordinate. One focus was on the entry span to the concave roller. The slopes were evaluated across the web width as the web exited roller R2, mid span, and finally at the exit of the span where the web enters roller R3. A second focus was the web in contact with the concave roller R3. The slope was evaluated across the web width as the web entered R3, half way through the angle of wrap and finally as the web exited R3.

The results are shown in Figure 13. In Figure 13a the results for the entry span are shown. Note that as the web enters the span and mid span that the slopes are non-zero. The fact that these slopes are non-zero at the exit of roller R2 indicates that slippage is occurring, probably the result of the short entry span length compared to the web width. It does appear that Swift's normal entry boundary condition may apply at the entry of the concave roller R3 at the end of the entering span. In Figure 13b the results for the web on the concave roller R3 are shown. It is clear that the slopes are near zero at the entry to R3 and mid-way through the wrap of R3. It is concluded that Swift's normal entry boundary condition [3] would be applicable for this particular web, concave roller and machine operating conditions. Note the slopes calculated as the web exits R3 are the highest seen in the simulation and indicative of the slippage occurring between the web and roller at that location.

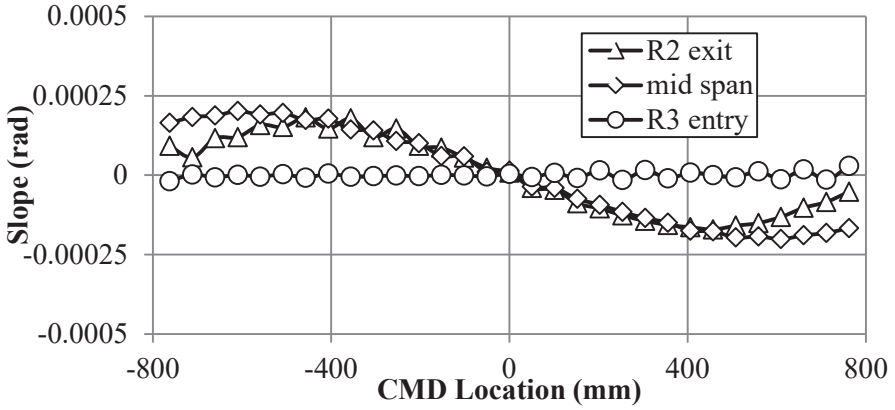

a) Comparison of Slope of Lateral Deformation in the Entry Span

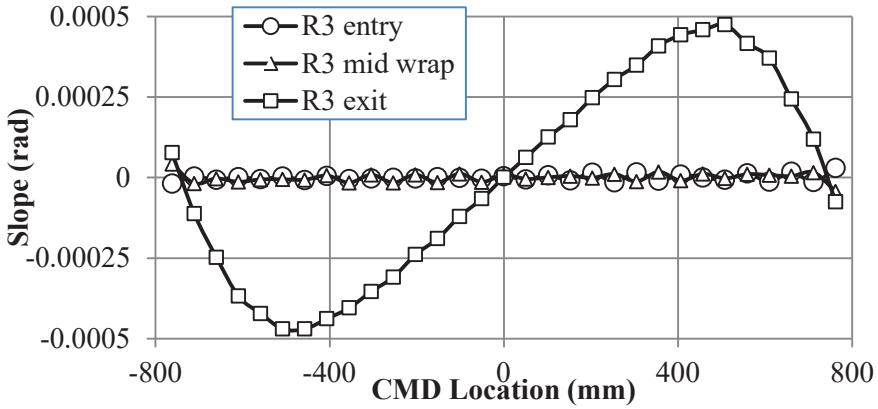

b) Comparison of Slope of Lateral Deformation on the Concave Roller

Figure 13 – Slope of Lateral Deformations for the Wide Web Case.

CONCLUSIONS

Explicit finite element modeling has been proven a useful method for the study of webs transiting concave rollers. A behavior that is evident in all the model results is a reversal in MD stress between the web entry and exit of the concave roller. MD stresses that are high at the web edges and low at the web center per expression {7} at the entry to the roller have become low at the edges and high at the web center when the web exits the roller. How this transition occurs depends entirely on the slippage which will depend case by case on roller concavity, the web to roller friction coefficient, the web thickness and modulus and web tension. For all the cases studied it was evident that the maximum spreading stress occurs as the web exits the concave roller at the web center. This behavior is the result of the MD stress near the web center rising toward the uniform stress level in the exiting span. The rise in MD tension is accompanied by a CMD contraction of the web that is resisted by friction and results in an increase in CMD spreading stress. For all cases studied it was found that the normal entry boundary condition was appropriate at the entry to the concave roller. There will be cases in which the friction forces will be inadequate to enforce this boundary condition. The slopes at the exit of the concave roller were non-zero as a result of the slippage in the MD and CMD directions. For the wide web case the slopes at the exit of the upstream roller R2 were found to be non-zero as a result of a short entry span length. It was also found that a device which is used for spreading webs is capable of buckling the web in the exit span.

REFERENCES

1. Lynch, R., "Web Handling Seminar Notes," Web Handling Research Center, 2011.
2. Hawkins, W. E., The Plastic Film and Foil Web Handling Guide, CRC Press, 2003.
3. Swift, H.W., "Camber for Belt Pulleys", Proceedings - Institute of Mechanical Engineers, June 1932.
4. Delahoussaye R.D. and Good J.K., "Analysis of Web Spreading Induced by the Concave Roller," Proceedings of the Second International Conference on Web Handling, Oklahoma State University, June 1993.

5. Swanson, R.P., "Testing and Analysis of Web Spreading and Anti-Wrinkle Devices," Proceedings of the Fourth International Conference on Web Handling, Oklahoma State University, June1997.
6. Markum, R.E. and Good, J.K., "Design of Contoured Rollers for Web Spreading," Proceedings of the Sixth International Conference on Web Handling, Oklahoma State University, June 2001.
7. Brown, J.L., "Effects of Concave Rollers, Curved Axis Rollers and Web Camber on the Deformation and Translation of a Moving Web," Proceedings of the Eighth International Conference on Web Handling, Oklahoma State University, June 2005.
8. Shelton, J. J., "Lateral Dynamics of a Moving Web," Ph. D. Thesis, Oklahoma State University, July 1968.
9. Kandadai, B. K. and Good, J. K., "Modeling Wound Rolls using Explicit FE Methods," Proceedings of the Ninth International Conference on Web Handling, Oklahoma State University, June 2007.
10. Abaqus Documentation, Dassault Systems, 2007.
11. Abaqus Documentation, ABAQUS Analysis Users Manual, Dassault Systems, 2009.
12. Beisel, J. A., and Good, J. K., "The Instability of Web in Transport," Journal of Applied Mechanics, ASME, Vol. 78, No 1, 2011.
13. Brown, J.L., "What FEA Analysis Can Tell Us About Spreaders," Applied Web Handling Conference, Minneapolis, MN, May, 2008.

Explicit Analysis of the Lateral Mechanics of Webs Transiting Concave Rollers	**S. Vaijapurkar & J. K. Good,** Oklahoma State University, USA

Name & Affiliation	**Question**
Neal Michal, Kimberly Clark	Fascinating paper. I appreciate your work. For a low modulus web, that has a lot of Poisson contraction in open spans, particularly if you have a lot of rollers, would you recommend that we should use negative crown rollers to offset the Poisson contraction? Would that be something that would be straight forward?
Name & Affiliation	**Answer**
Keith Good, Oklahoma State University	The concave roller is an aggressive spreader. It works well over a broad spectrum of friction coefficients. When I offer something for an industrial setting, you always worry about how robust it is and how it works in different applications. I would say that it's a very effective spreader, but when I consider low modulus webs I immediately start thinking viscoelasticity at the same time. The concave roller stretches the edge of the web in the MD while it spreads the web in the CMD. Stretching the edges of viscoelastic web may produce a baggy edged web if the concavity is too aggressive. The concavity should be chosen carefully.
Name & Affiliation	**Question**
Dave Roisum, Finishing Technologies, Inc.	I think one ideal for many situations would be a spreader without a spreading profile. In other words, a CMD stresses relatively uniform across the width. I am wondering if you could adjust that parabolic profile to get rid of some of that highly nonuniform spreading we are seeing?
Name & Affiliation	**Answer**
Keith Good, Oklahoma State University	I think it is possible and you can give the analytical surface any contour you want in the analysis. That's part of the power of the method. That is possible, but I would have to say if you are looking at a web line that has to run 10 different products, there might not be one concave profile that is optimal for all products.
Name & Affiliation	**Question**
Kevin Cole, Optimation Technology, Inc.	I have one question about the entry span. You did show shear stresses on either edge. We know with tapered rollers, we have the risk of web troughs for low tapers and then wrinkles with higher tapers. Could there be a situation where even though you have spreading and positive CMD tension in the center of the web that you could get too much shear and perhaps form wrinkles and troughs?
Name & Affiliation	**Answer**
Keith Good, Oklahoma State University	In the way in which you have cast the question I would say no. In Figures 7, 9, and 12b positive CMD stresses are shown across the entire web width. As long as these stresses are tensile troughs and wrinkles cannot form. Yes

there are shear stresses due to the velocity variation associated from the concavity. These shear stresses are quite different from those shear stresses that are due to lateral steering forces from a tapered roller. Our simulations demonstrated it was possible to generate troughs in the exit span of a concave roller but not in the entry span.

Name & Affiliation	Question
Kevin Cole, Optimation Technology, Inc.	Do you think you could ever get troughs or wrinkles at the entry to the concave roller?
Name & Affiliation	**Answer**
Keith Good, Oklahoma State University	Yes. I believe it is possible to generate enough entrained air due to high web velocity possibly combined with low web tension that the MD and shear stress distributions that result from friction forces between the concave roller and web are lost. Normal entry is no longer ensured and if the concave roller is an idler the surface velocity of the roller may drop beneath that of the web. In such situations the web may trough in the entry span and wrinkle on the concave roller. There is also certain minimum web tension that will ensure complete contact between the web and concave roller that was introduced in a 2001 IWEB paper by Ron Markum and me. This minimum tension depends on web width, the degree of concavity and the web modulus. Web tensions less than the minimum value will result in separation between the web and the concave roller surface and may result in troughs in the entry span and wrinkles on the roller. The web must be frictionally engaged with the concave roller to achieve spreading. Finally all of our analyses are for cases where the CMD centers of the web and the concave roller are coincident. I believe it is possible to have a lateral disturbance in the form of a splice that could induce dynamic lateral instability in the web and produce limit cycle behavior. In such cases dynamic shears will exist in the web that could produce troughs and possibly wrinkles.
Name & Affiliation	**Question**
Bob Lucas, Winder Science	When dealing with webs such as photographic film and others, scratches are serious issues. Some of the premium gloss paper grades we have used in times past in scratch analysis to determine what rolls were slipping, etc. We set up a detailed procedure for understanding traction and whether or not a web is slipping on a given roll. You were commenting on some of your presentation about slippage in both directions - machine direction and cross-machine direction. Have you seen any evidence of scratches at a diagonal?

Name & Affiliation	Answer
Keith Good, Oklahoma State University	The contact shear stresses at the exit of the concave roller shown in Figure 10 have MD and CMD components that have the same range. That being said, note there are locations where the contact shear stress in the MD direction are minimal while the CMD component is maximum. There are other locations where the opposite is true and a host of other behaviors in between. This provides evidence that the micro-scratches could take on a number of different directions across the web width.
Name & Affiliation	**Question**
Bob Lucas, Winder Science	I wonder if it might be worth having an intentional pick line on the roll with the specific intent of trying to create a scratch to document whether or not you have motion.
Name & Affiliation	**Answer**
Keith Good, Oklahoma State University	The relative motion between the web and the roller surfaces is captured in the current output databases from the explicit analyses. We can document the direction and magnitude of this relative motion which could potentially generate scratches.
Name & Affiliation	**Question**
Günther Brandenburg, Technische Universität München	Did you investigate convex rollers? This would be interesting to know.
Name & Affiliation	**Answer**
Keith Good, Oklahoma State University	We have looked at those in the past. Convex rollers, sometimes called crown rollers, are not favored in the web handling industry because they tend to wrinkle webs. Crowned rollers are of historical interest because of the line shafting and belts that were used to transmit power from the beginning of the industrial revolution. Yes, I have studied the convex rollers briefly, but not to the detail that we've studied the concave roller.
Name & Affiliation	**Comment**
John Shelton, Oklahoma State University	Scratching at an angle or scratch marks that are little hooks or curves are seen in orienters. The Brueckner people here have seen such things more than I have. It may be something could be learned about scratching in more than one direction from the orientation. I thought that might be interesting.